



Published in final edited form as:

Biol Psychiatry. 2019 February 01; 85(3): 226–236. doi:10.1016/j.biopsych.2018.08.020.

Alpha1 and beta3 adrenergic receptor-mediated mesolimbic homeostatic plasticity confers resilience to social stress in susceptible mice

Hongxing Zhang^{1,2,3}, Dipesh Chaudhury^{1,4}, Alexander R. Nectow^{5,6}, Allyson K. Friedman¹, Song Zhang^{1,2,3}, Barbara Juarez^{1,7,8}, He Liu^{2,3,4}, Madeline L. Pfau⁷, Hossein Aleyasin^{7,9}, Cheng Jiang⁷, Marshall Crumiller¹⁰, Erin S. Calipari⁷, Stacy M. Ku^{1,7}, Carole Morel¹, Nikos Tzavaras¹¹, Sarah E. Montgomery¹, Michelle He¹, Stephen R. Salton⁷, Scott J. Russo^{7,9}, Eric J. Nestler⁷, Jeffrey M. Friedman^{5,6}, Jun-Li Cao^{2,3,12,*}, Ming-Hu Han^{1,7,9,*}

¹Department of Pharmacological Sciences, Institute for Systems Biomedicine, Icahn school of Medicine at Mount Sinai, New York, New York, USA, 10029-6574

²Jiangsu Province Key Laboratory of Anesthesiology, Xuzhou Medical University, Xuzhou, Jiangsu, China, 221004

³Jiangsu Province Key Laboratory of Anesthesia and Analgesia Application Technology, Xuzhou Medical University, Xuzhou, Jiangsu, China, 221004

⁴Division of Science, New York University Abu Dhabi (NYUAD), Saadiyat Island, Abu Dhabi, United Arab Emirates, 129188

⁵Laboratory of Molecular Genetics, The Rockefeller University, New York, NY, USA, 10065

⁶Howard Hughes Medical Institute, Chevy Chase, Maryland, USA, 20815

⁷Fishberg Department of Neuroscience, Friedman Brain Institute, Icahn school of Medicine at Mount Sinai, New York, New York, USA, 10029-6574

⁸Department of Pharmacology, University of Washington, Seattle, WA, USA, 98195

⁹Center for Affective Neuroscience, Friedman Brain Institute, Icahn school of Medicine at Mount Sinai, New York, New York, USA, 10029-6574

¹⁰Laboratory of Biophysics, The Rockefeller University, New York, New York, USA, 10065

¹¹Microscopy CORE, Icahn School of Medicine at Mount Sinai, New York, New York, USA, 10029-6574

*Corresponding authors: **Jun-Li Cao**: Jiangsu Province Key Laboratory of Anesthesiology, Xuzhou Medical University, Xuzhou 221004, China; Telephone: 86-516-83262686; caojl0310@aliyun.com. **Ming-Hu Han**: Department of Pharmacological Sciences, Institute for Systems Biomedicine, Icahn school of Medicine at Mount Sinai, New York, New York 10029, USA; Telephone: 212-659-1792; ming-hu.han@mssm.edu.

Publisher's Disclaimer: This is a PDF file of an unedited manuscript that has been accepted for publication. As a service to our customers we are providing this early version of the manuscript. The manuscript will undergo copyediting, typesetting, and review of the resulting proof before it is published in its final citable form. Please note that during the production process errors may be discovered which could affect the content, and all legal disclaimers that apply to the journal pertain.

DISCLOSURES

All authors reported no biomedical financial interests or potential conflicts of interest.

¹²Department of Anesthesiology, the Affiliated Hospital of Xuzhou Medical University, Xuzhou, Jiangsu, China, 221002

Abstract

BACKGROUND: Homeostatic plasticity in mesolimbic dopamine (DA) neurons plays an essential role in mediating resilience to social stress. Recent evidence implicates an association between stress resilience and projections from the locus coeruleus to the ventral tegmental area (LC→VTA) DA system. However, the precise circuitry and molecular mechanisms of the homeostatic plasticity in mesolimbic DA neurons mediated by the LC→VTA circuitry, and its role in conferring resilience to social defeat stress, have not been described.

METHODS: In a well-established chronic social defeat stress (CSDS) model of depression, using projection-specific electrophysiological recordings, optogenetic, pharmacological, and molecular profiling techniques, we investigated the functional role and molecular basis of an LC→VTA circuit in conferring resilience to social defeat stress.

RESULTS: We found that LC neurons projecting to the VTA exhibit enhanced firing activity in resilient, but not susceptible, mice. Optogenetically mimicking this firing adaptation in susceptible mice reverses their depression-related behaviors, and induces reversal of cellular hyperactivity and homeostatic plasticity in VTA DA neurons projecting to nucleus accumbens (NAc). Circuit-specific molecular profiling studies reveal that $\alpha 1$ and $\beta 3$ adrenergic receptors are highly expressed in VTA→NAc DA neurons. Pharmacologically activating these receptors induces similar pro-resilient effects at the ion channel, cellular and behavioral levels, whereas antagonizing these receptors blocks the pro-resilient effect of optogenetic activation of LC→VTA circuit neurons in susceptible mice.

CONCLUSIONS: These findings reveal a key role of the LC→VTA circuit in mediating homeostatic plasticity in stress resilience, and reveal $\alpha 1$ and $\beta 3$ adrenergic receptors as new molecular targets for therapeutically promoting resilience.

Keywords

Locus coeruleus; Ventral tegmental area; Nucleus accumbens; Adrenergic receptors; Depression; Resilience

Recently, a growing body of studies has begun to pay attention to how some individuals maintain seemingly unaltered psychophysiological functioning (resilient to depression), while others are more susceptible when they experience stress (1, 2).

Resilience is defined as “the process of adapting well in the face of adversity, trauma, tragedy, threats or even significant sources of threat” (3). By achieving beneficial adaptations, resilient individuals are able to survive and even thrive despite exposure to high levels of adversity, such as prolonged severe stress (1, 2, 4, 5). Investigating resilient mechanisms in the brain becomes important because such studies could provide a conceptually novel strategy to treat stress-related illnesses by promoting mechanisms of natural resilience(2). However, in contrast to stress-induced pathological alterations, less is known about the neural mechanisms that underlie beneficial adaptations for resilience in the

brain. Recent investigations demonstrate that resilient individuals actively use more genes to cope with stress and establish stable neural adaptations (5-7). Further, and an increasing number of studies has begun to reveal the important neural mechanisms of such active resilience (1, 8-12). More recent work has uncovered a physiological role of VTA→NAc DA neurons in resilience versus susceptible behavioral phenotypes in the chronic social defeat stress (CSDS) model of depression (10, 11, 13). Moreover, a homeostatic plasticity—a new balance between I_h current (hyperpolarization-activated cation channel current) and potassium (K^+) channel currents—in mesolimbic DA neurons mediates active resilience to CSDS (11). However, how upstream brain regions control these pathway-specific DA neurons to establish resilient adaptations and reverse depressive-like behaviors in susceptible animals remains unknown.

The LC, a norepinephrine (NE) producing nucleus of the brainstem is important for modulating vigilance (14), arousal (15), cognition (16), sleep/awake transitions (17) and drug addiction (18). The LC has also been implicated in stress resilience in both humans and rodent models (4, 19, 20). One of the key downstream brain regions of LC neurons is the VTA. Recently, it has been revealed that resilient mice had an increase in NE release from LC neurons that project to the VTA (21), implicating the role of NE in the VTA in mood regulation. In the present study, we examined whether LC→VTA circuit neurons mediate the homeostatic plasticity mechanisms in mesolimbic DA neurons and investigated which adrenergic receptors mediate this resilience plasticity.

METHODS AND MATERIALS

Animals

Male 7-week-old C57BL/6J (Jackson Laboratory) and CD1 retired breeders (Charles River) were used to perform the chronic social defeat stress paradigm. Ten-week-old DAT-IRES-Cre knock-in mice (22) were used to determine the gene expression of adrenergic receptors in projection-specific VTA DA neurons using the circuit-mapping molecular profiling technique Retro-TRAP (23, 24). All mice were singly housed on a 12 hour light-dark schedule with food and water available *ad libitum*.

Chronic social defeat stress (CSDS) paradigm

CSDS was performed according to published protocols (6, 10, 11, 13, 25, 26) and is described in Supplementary Materials.

Social interaction test

Social interaction tests were performed on day 11 or following related pharmacological and optogenetic treatments which were performed in the study as described in Supplementary Materials and as described previously (6, 10, 11, 25, 26).

Ex vivo electrophysiology

Mice were anaesthetized with isoflurane and perfused immediately with ice-cold aCSF (artificial cerebrospinal fluid), which contained (in mM): 128 NaCl, 3 KCl, 1.25 NaH_2PO_4 , 10 D-glucose, 24 NaHCO_3 , 2 CaCl_2 and 2 MgCl_2 (oxygenated with 95% O_2 and 5% CO_2 ,

pH 7.4, 295–305 mOsm). Cell-attached and whole-cell patch-clamp recording were performed in acute brain slices containing LC or VTA as reported in our previous studies (10, 11, 25).

***In vivo* single-unit electrophysiological recording**

As we previously reported, mice were anesthetized with 10% chloral hydrate (400 mg/kg), and heads were fixed onto a stereotaxic frame horizontally (25). Using bregma, LC was located within the range (in mm): anterior/posterior: –5.30 to –5.50, medial/lateral: 0.50 to 1.20, dorsal/ventral: –2.70 to –4.00. Glass micropipettes (15–20 M Ω) filled with 2M NaCl were used for recording. LC neurons were identified with criteria reported in previous studies (27, 28).

Molecular profiling

DAT-IRES-Cre mice were injected in the NAc with CAV-GFP (0.5 μ l, coordinates: \pm 1.0 mm ML, +1.35 mm AP, \pm 4.2 mm DV), as well as in the VTA with AAV-IV-NBL10 (0.5 μ l, coordinates: \pm 0.5 mm ML, \pm 3.15 mm AP, \pm 4.2 mm DV). Fifteen days after injections, mice were sacrificed and the VTA was rapidly dissected on ice. Briefly, a 2 mm slice was made approximately covering the region 2–4 mm posterior to bregma. Brains were then pooled into three groups of six mice per group, homogenized in the presence of recombinant nanobody (100 ng/ml, ChromoTek), and centrifuged to clarify. GFP Immunoprecipitation was performed with two mouse monoclonal antibodies (19C8, 19F7; (29)) according to previous protocols (23, 24). The resulting RNA was purified using the Absolutely RNA Nanoprep Kit (Agilent) and analyzed using an Agilent 2100 Bioanalyzer, followed by reverse transcription (QIAGEN QuantiTect) and Taqman qPCR. Gene expression was normalized to large ribosomal protein gene 123 (rp123) (23).

Statistics

Data are presented as mean \pm s.e.m. All analyses were performed with Prism software. Normality of the data was statistically tested by the D'Agostino-Pearson omnibus normality test. Normally distributed data from multiple-groups were compared with one-way analysis of variance with/without repeated factors (*one-way ANOVA*), followed by a *post-hoc Bonferroni's multiple comparison test* when appropriate. Data that did not pass the normality test was analyzed by a nonparametric testing (*Kruskal-Willis test* followed by *Dunn's multiple comparisons test*). Adrenergic receptor genes expression ratio were compared with a paired Student's t test. Statistical significance was set at $P < 0.05$.

RESULTS

LC→VTA NE neurons display enhanced firing activity in resilient mice

Taking advantage of a well-established chronic (10-day) social defeat stress model of depression (6, 10–12), we segregated susceptible and resilient mice based on their social interaction (SI) test behavior: susceptible mice display profound social avoidance, a behavior that was absent in resilient mice despite exposure to equivalent stress (Figure 1A, B; Figure S1 and S2). Resilient mice also lack other depressive behaviors that are displayed in susceptible mice (1, 10, 11, 13). To assess possible changes in the firing activity of LC

neurons, we carried out *in vivo* single unit recordings from anesthetized stress-naïve control, susceptible and resilient mice to measure both firing rate and bursting (phasic) properties (30) (Figure 1C, D). We observed that the *in vivo* firing rate and bursting frequency (per 100 s) of LC neurons were significantly increased in the resilient mice when compared to control and susceptible mice, with no change observed in spike number per burst event (Figure 1E-G). There was also a trend for an increase in the percentage of spikes found in a burst and time spent bursting in the resilient mice as compared to control and susceptible mice (Supplementary Figure S3).

Next, we tested whether the firing changes observed in the LC neurons of resilient mice have projection-target specificity. To label specific projections and measure the baseline firing of these circuit neurons in an *ex vivo* slice preparation (18, 31, 32), we injected a retrograde green Lumafluor into the VTA and a retrograde red Lumafluor into the medial prefrontal cortex (mPFC) (Figure 1H-J). These two brain regions are well known to contribute to the segregation of the susceptible and resilience phenotypes, respectively (6, 9, 11, 33, 34). Interestingly, we found that only 3.5% of LC neurons co-labeled with both red and green Lumafluors (Figure S4 A and B), suggesting that the majority of LC→VTA and LC→mPFC projection neurons are distinct subpopulations. Furthermore, our *ex vivo* slice recordings show that LC→VTA neurons (green, ~98% are tyrosine hydroxylase positive, Figure S4 C and D) exhibited increased firing in resilient mice when compared to control and susceptible groups, with no difference observed for firing frequencies in LC→mPFC neurons (Figure 1K, L). Unexpectedly, unlabeled LC neurons displayed firing rates comparable to control (Figure 1M), suggesting that firing alterations may be specific to LC→VTA projecting neurons.

We subsequently focused on the LC→VTA projection pathway because of its crucial role in segregating susceptible and resilient phenotypes (6). Moreover, our previous work demonstrated signature adaptations in VTA DA neurons projecting to the NAc that drive resilience (11). Therefore, we hypothesized that the increased firing adaptation in the LC→VTA circuit may contribute significantly to resilience mechanisms observed in the VTA.

Repeated optical activation of LC→VTA neurons promotes resilience in susceptible mice

To investigate the relationship between the firing alterations of LC→VTA neurons and behavioral outcomes, we utilized a combination of viral and optogenetic techniques (11, 13). To specifically target the LC→VTA pathway, we injected a retrograde AAV2/5-Cre into the VTA, and Cre-inducible AAV5-DIO-ChR2-eYFP into the LC to selectively express ChR2 in LC→VTA neurons (AAV5-DIO-eYFP as control) (Figure 2A, B). We confirmed that optical phasic stimulation (5 pulses/10 ms pulse width) of *ex vivo* LC→VTA neurons reliably induced five spikes and photocurrents in whole-cell current- and voltage-clamp modes, respectively (Figure S5A, B). With this confirmation, we performed these dual injection surgeries before the onset of chronic social defeat stress. Following the defeat paradigm and the first SI test, susceptible and stress-naïve control mice were implanted with an optical fiber (ferrule) placed above the LC for selective stimulation of ChR2-expressing LC→VTA neurons (Figure S6). After recovery, we delivered *in vivo* optical phasic stimulation to

LC→VTA neurons for 5 minutes during a second SI test, and failed to observe significant effects on social avoidance behavior (Figure 2D; Figure S7). We then turned to chronic stimulations to determine if repeated activation (20 minutes per day for 5 days or 10 days) of the LC→VTA circuit could reverse depressive-like behaviors (Figure 2A-C). Our data show that eYFP expressing susceptible mice continue to display profound and stable avoidant behavior when compared to control mice (Figure 2E, F), and to themselves across repeated SI tests (for time in interaction zone, *two-way ANOVA* followed by *post-hoc Bonferroni's test*, Target: SI^{Figure 2D} vs. SI^{Figure 2E}, $P > 0.9999$, SI^{Figure 2D} vs. SI^{Figure 2F}, $P = 0.4200$, SI^{Figure 2E} vs. SI^{Figure 2F}, $P > 0.9999$). However, the avoidant behaviors of Chr2 expressing susceptible mice were reversed following 5 days (Figure 2E; Figure S8A) and 10 days (Figure 2F; Figure S9A) of LC→VTA stimulation, without affecting locomotor activity during the social interaction tests (Figure S8B, C; Figure S9B, C). The 10-day optical stimulation of LC→VTA neurons also significantly increased sucrose preference, and tended to decrease immobility in a forced swim test (Figure 2G, H; Figure S10), further demonstrating pro-resilient effects. These results support the view that repeated activation of the LC→VTA circuit promotes resilience and beneficially reverses behavioral abnormalities in otherwise susceptible mice.

Repeated optical activation of LC→VTA neurons in susceptible mice enhances the firing activity of LC neurons

To further investigate the cellular mechanisms that underlie the pro-resilience effects following 10-day optical stimulation of LC→VTA circuit, we examined alterations in LC neurons and their downstream targets in VTA DA neurons. We first confirmed the behavioral phenotypes in a new cohort of socially defeated mice (Figure S11), and then carried out *in vivo* single unit recordings from LC neurons (continuing the stimulation 20-minute/day until the day of *in vivo* recordings as shown in Figure 3A and B). Our data demonstrates that repeated optical stimulation of LC→VTA neurons increased the *in vivo* firing rate and bursting frequency of LC neurons (when compared to the absence of optical stimulation), with no change observed in spike number per bursting event, when compared to control (Figure 3C-E). There is a significant increase or a trend of increase in percentages of bursting spikes and time in burst in the optically stimulated group as compared to control (Figure S12). These results induced by repeated LC→VTA optical activation are similar to the *in vivo* recordings observed in naturally resilient mice.

Repeated optical activation of LC→VTA neurons in susceptible mice induces homeostatic plasticity in VTA→NAc DA neurons

To examine whether repeated optical stimulation of LC→VTA induces downstream changes in the VTA, we focused on VTA DA neurons projecting to the NAc, the subpopulation of these neurons that display signature homeostatic adaptations in I_h current and K^+ channel currents in resilient mice and that mediate behavioral resilience (11). These channels establish a critical intrinsic balance to maintain control levels of firing in the VTA→NAc DA neurons of resilient mice as compared to the pathological increase in firing seen in susceptible mice (11). To test whether repeated optical stimulation of the LC→VTA circuit has an effect on the firing rate and balance in intrinsic currents balance of VTA→NAc DA neurons, we labeled VTA→NAc neurons by injecting retrograde red Luminafluors into the

NAc, and expressed ChR2 selectively in LC→VTA neurons (Figure 4A, B). We delivered 10-day *in vivo* optical stimulation to LC→VTA neurons in the LC as stated above, to reverse social avoidance (Figure S13), and measured the firing rates and ionic currents from VTA→NAc putative DA neurons (large I_h current and >1.1 ms triphasic waveform, Figure S14) of control, susceptible-eYFP and susceptible-ChR2 groups. Our data show that 10-day optical stimulation of LC→VTA neurons completely reversed the pathological hyperactivity observed in the susceptible-eYFP group (Figure 3C), and achieved an intrinsic currents balance similar to that observed in resilient mice (Figure 4D-E). These results demonstrate that mimicking the resilience-associated firing adaptation in the LC→VTA circuit by repeatedly activating this circuit's neurons induces key resilience adaptations in VTA→NAc neurons.

VTA $\alpha 1$ and $\beta 3$ adrenergic receptors promotes resilience and intrinsic currents balance in VTA→NAc DA neurons in susceptible mice

Our next question was which adrenergic receptors in the VTA mediate these effects. To perform molecular profiling of adrenergic receptors in VTA→NAc DA neurons, we injected retrograde tracer CAV-GFP into the NAc and Cre-inducible AAV-FLEX-NBL10 into the VTA of stress-naive DAT-IRES-Cre mice (Figure 5A, B). Immunostaining validation shows a substantial number of VTA→NAc DA neurons targeted by this approach (Figure S15). Our profiling data revealed that, among adrenergic receptor subunits, $\alpha 1$ and $\beta 3$ were most highly expressed in VTA→NAc DA neurons as compared to their expression levels in all VTA DA neurons (Figure 5C).

We further tested whether $\alpha 1$ and $\beta 3$ receptors are involved in mediating the resilience behavior and intrinsic currents balance induced by LC→VTA activation in the VTA→NAc circuit. Following chronic social defeat stress, we injected a red Lumafluor into the NAc to label VTA→NAc neurons, and locally infused $\alpha 1$ and $\beta 3$ receptor agonists (methoxamine HCl and CL316243) into the VTA for 10 days and then performed a SI test to measure social avoidance behavior (Figure 5D E). We observed that 10-day intra-VTA infusion of this cocktail completely reversed social avoidant behaviors in susceptible mice when compared to vehicle-infused susceptible mice (Figure 5F; Figure S16). We then performed *ex vivo* recordings to determine the cellular alterations within red Lumafluor labeled VTA→NAc neurons following chronic infusions. Repeated infusion of $\alpha 1$ and $\beta 3$ receptor agonists reversed the pathological hyperactivity of VTA→NAc neurons that is associated with susceptibility (Figure 5G). Moreover, these infusions increased I_h and K^+ currents of lumafluor-labeled VTA→NAc neurons as compared to susceptible-vehicle control (Figure 5H, I), reflecting the balance in intrinsic currents associated with natural resilience. These findings indicate that activation of these adrenergic receptors is sufficient to induce a resilience-like phenotype at the ion channel, cellular and behavioral levels.

VTA $\alpha 1$ and $\beta 3$ adrenergic receptors are necessary for the pro-resilience effect of repeated optical stimulation of LC→VTA neurons

To further study this mechanism, we investigated whether antagonists of $\alpha 1$ and $\beta 3$ receptors block the pro-resilience effects induced by optical stimulation of LC→VTA neurons. We expressed ChR2 in LC→VTA neurons as stated above and delivered 10-day

optical stimulation to LC→VTA neurons of susceptible mice with intra-VTA infusion of $\alpha 1$ and $\beta 3$ antagonists (cyclazosin and SR59230A HCl) (Figure 6A, B). Such intra-VTA infusions (once a day for 10 days) completely blocked the optical stimulation-induced reversal of social avoidance behavior as compared to mice receiving vehicle (Figure 6 C; Figure S17), demonstrating that these receptors are necessary for the pro-resilience effects of optical stimulation of the LC→VTA circuit.

DISCUSSION

This study showed that (1) the firing activity of LC→VTA neurons is increased exclusively in resilient, but not susceptible, mice after CSDS; (2) optogenetically mimicking this adaptive change (activating LC→VTA neurons) in stress-exposed susceptible mice promotes a resilience-like phenotype, including reversal of hyperactivity of VTA→NAc DA neurons, homeostatic plasticity (intrinsic balance between I_h current and K^+ currents) and normalization of social behavior; (3) molecular profiling and pharmacological studies identify $\alpha 1$ and $\beta 3$ adrenergic receptors expressed by VTA DA neurons as being sufficient and necessary to induce resilience-like phenotypes. Overall, these circuit-specific investigations demonstrate that the LC→VTA→NAc pathway plays an important role in promoting resilience through norepinephrine mechanisms in the VTA.

We recently demonstrated that VTA→NAc DA neurons constitute a neural circuit in which a resilience-specific active form of homeostatic plasticity is established by an intrinsic balance of I_h current and K^+ currents to maintain normal neuronal activity as well as behavioral resilience (11). Following this finding, we further identified KCNQ-type K^+ channels as a target for conceptually novel antidepressants that function through the potentiation of active resilience mechanisms (35). Recently, researchers have started to investigate the extrinsic synaptic mechanisms that underlie this active homeostatic plasticity (21, 36). It is well known that VTA DA neurons are regulated by intrinsic ion channels, and extrinsic synaptic innervation, including a heavy noradrenergic input from the LC (37-39). Our results in this study consistently support these early findings that the LC-NE system plays an important role in mediating resilience in human and animal models (4, 21, 40).

It is widely known that the LC-NE neurons respond to stress by globally priming neurons in the brain (4, 31, 41-46). Increasing evidence has also shows the heterogeneity of LC-NE neurons (46-49), as seen for VTA DA neurons (10, 11, 50, 51). Here, our *in vitro* electrophysiological experiments showed that LC→VTA neurons fired significantly higher in the resilient subgroup as compared to stress-naïve control mice, while LC→VTA neurons of susceptible mice have a normal firing activity comparable to that of control mice. Our *in vivo* recording data further confirmed that LC neurons from resilient mice displayed enhanced firing rates and phasic firing events as compared to control and susceptible mice, which is consistent with a recent study reporting greater NE release in the VTA of resilient mice (21). These findings indicated that hyperactivity of LC→VTA neurons might be an important hallmark of resilience in the brain. Hyperactivity of the LC-NE neurons has been implicated in mediating hyper-responsiveness, including increased vigilance, in posttraumatic stress disorder (PTSD) and arousal dysfunction (15, 52). In our previous study using the CSDS model, we also observed elevated arousal in both susceptible and resilient

mice (6), suggesting that increased arousal might be related to the development of stress susceptibility versus resilience depending on the timing of the vigilance. Greater vigilance before stressor exposure, as an active function, might promote resilience, whereas increased vigilance induced by stress, for example, hyper-responsiveness in PTSD, would be passive and pathological. It would be very interesting to investigate the role for vigilance in stress resilience in future work, and it is possible that high levels of natural vigilance acts as a predictor of stress resilience.

Our *in vivo* optogenetic investigations confirmed that 5 or 10 days of repeatedly activating these neural circuit neurons was sufficient to reverse social avoidance in previously defined susceptible mice. Strikingly, this stimulation also induced homeostatic plasticity of VTA→NAc DA neurons, a featured self-tuning adaptive balance between I_h current and K^+ currents that is uniquely seen in resilient mice. In addition, this same stimulation consistently stabilized the firing activity and normalized social behavior. Interestingly, we observed that the firing variation in LC→mPFC circuit neurons is much greater than that in LC→VTA circuit neurons. We are not sure whether this indicates that different subgroups of LC→mPFC neurons that play a distinct functional roles in the response to social stress. In future work, it would be interesting to explore the functional role of other LC-related circuits, including LC→mPFC neurons, in mediating stress resilience versus susceptibility.

VTA DA neurons express multiple kinds of adrenergic receptors that might mediate the interaction between the LC-NE inputs and VTA-DA neurons. Taking advantage of a circuit- and cell type-specific molecular profiling technique (23), we identified enrichment of $\alpha 1$ and $\beta 3$ adrenergic receptors in VTA→NAc DA neurons, and found that repeated pharmacological activation of VTA $\alpha 1$ and $\beta 3$ adrenergic receptors with a cocktail of specific agonists reversed social avoidance behavior in previously identified susceptible mice. Strikingly, this treatment also completely normalized the pathological hyperactivity of VTA→NAc DA neurons and established a resilience-like intrinsic balance between I_h and K^+ currents, a critically important mechanism of homeostatic plasticity identified in naturally resilient mice and in susceptible animals after repeated optogenetic stimulation (11). These findings indicate that repeated activation of VTA $\alpha 1$ and $\beta 3$ adrenergic receptors, and repeated activation of LC→VTA neurons, display similar pro-resilient effects in susceptible mice at the cellular and behavioral levels. This interesting phenomenon suggests that $\alpha 1$ and $\beta 3$ adrenergic receptors might be key mediators of the synaptic relay between the LC-NE system and the VTA→NAc reward circuit. As expected, we observed that pretreatment with $\alpha 1$ and $\beta 3$ receptor antagonists is sufficient to abolish the pro-resilience of repeated optogenetic activation of LC→VTA neurons in the social interaction test. This study thereby establishes that $\alpha 1$ and $\beta 3$ receptors are necessary for the pro-resilient effects of LC-NE on VTA→NAc DA neurons. Another important finding of this study is that it introduces a novel extrinsic mechanism that accounts for the homeostatic plasticity in VTA→NAc DA neurons that is associated with resilience. In these studies, we combined pharmacological agonist and antagonist treatments for both adrenergic receptors to maximize our ability to detect their roles. Future studies are needed to examine whether manipulation of either receptor alone would be sufficient to induce antidepressant-like behavioral effects.

While the CSDS paradigm is a well-established and widely used rodent model of depression, our previous study (6) showed that socially defeated mice also exhibit anxiety-like phenotypes. In the present study, we reported that activation of LC→VTA circuit reversed deficits in social behavior and forced swim performance. It is not completely clear whether or not the reversal of these deficits was induced by normalizing depression- or an anxiety-related components because social interaction and forced swim tests that we used in this study may include both components (53). Our results from the sucrose preference test suggest that depression components may contribute, at least in part, to the reversal effects observed. Nevertheless, the functional role of LC→VTA in the regulation of an anxiety phenotype in the context of CSDS needs to be explored in greater depth in the future.

Ketamine is used routinely for surgical anesthesia in rodents. There is now robust evidence that a single sub-anesthetic dose of ketamine produces rapid antidepressant effects in humans and animals (54, 55). However, there has been no evidence so far showing that ketamine at anesthetic doses such as 100 mg/kg in our case, which is far higher than used for depression treatment, has any antidepressant effect (6, 10, 11, 13, 25, 35). Nevertheless, this caveat should be considered when interpreting data from animals that underwent ketamine-induced anesthesia.

Collectively, these observations provide highly consistent molecular, cellular and behavioral evidence for the underlying mechanisms by which an LC→VTA→NAc circuit functions as a stress resilient pathway in the brain. Specifically, these results establish $\alpha 1$ and $\beta 3$ adrenergic receptors as new molecular targets for therapeutically promoting natural resilience, a possibility which now warrants clinical testing, while current research focuses on obtaining a more complete understanding of the mechanisms of natural resilience.

Supplementary Material

Refer to Web version on PubMed Central for supplementary material.

ACKNOWLEDGMENTS

This work was supported by the National Institute of Mental Health (R01 MH092306: M.H.H.; R01 MH051399: E.J.N.), National Natural Science Foundation of China (NSFC81230025, 81720108013: J.L.C.; NSFC81200862, 81771453: H.Z.), Jiangsu Province Natural Science Foundation (BK20171158: H.Z.), Xuzhou Medical University Start-up Grant for Excellent Talents (D2018010: H.Z.), National Research Service Award (F31 AA022862, T32 MH 087004: B.J.; F32 MH096464: A.K.F.), Johnson & Johnson/IMHRO Rising Star Translational Research Award (M.H.H.), and NARSAD Independent Investigator Award (M.H.H.). The Jiangsu Provincial Special Program of Medical Science Grant No. BL2014029; the Priority Academic Program Development of Jiangsu Higher Education Institutions.

References:

1. Russo SJ, Murrough JW, Han MH, Charney DS, Nestler EJ (2012): Neurobiology of resilience. *Nature neuroscience*. 15:1475–1484. [PubMed: 23064380]
2. Han MH, Nestler EJ (2017): Neural Substrates of Depression and Resilience. *Neurotherapeutics: the journal of the American Society for Experimental NeuroTherapeutics*. 14:677–686. [PubMed: 28397115]
3. American Psychological Association (2014): *The Road to Resilience*. Washington DC: American Psychological Association <http://www.apa.org/helpcenter/road-resilience.aspx>.

4. Charney DS (2004): Psychobiological mechanisms of resilience and vulnerability: implications for successful adaptation to extreme stress. *The American journal of psychiatry*. 161:195–216. [PubMed: 14754765]
5. Feder A, Nestler EJ, Charney DS (2009): Psychobiology and molecular genetics of resilience. *Nature reviews Neuroscience*. 10:446–457. [PubMed: 19455174]
6. Krishnan V, Han MH, Graham DL, Berton O, Renthal W, Russo SJ, et al. (2007): Molecular adaptations underlying susceptibility and resistance to social defeat in brain reward regions. *Cell*. 131:391–404. [PubMed: 17956738]
7. Bagot RC, Cates HM, Purushothaman I, Lorsch ZS, Walker DM, Wang J, et al. (2016): Circuit-wide Transcriptional Profiling Reveals Brain Region-Specific Gene Networks Regulating Depression Susceptibility. *Neuron*. 90:969–983. [PubMed: 27181059]
8. Berton O, Covington HE 3rd, Ebner K, Tsankova NM, Carle TL, Ulery P, et al. (2007): Induction of deltaFosB in the periaqueductal gray by stress promotes active coping responses. *Neuron*. 55:289–300. [PubMed: 17640529]
9. Vialou V, Robison AJ, Laplant QC, Covington HE 3rd, Dietz DM, Ohnishi YN, et al. (2010): DeltaFosB in brain reward circuits mediates resilience to stress and antidepressant responses. *Nat Neurosci*. 13:745–752. [PubMed: 20473292]
10. Chaudhury D, Walsh JJ, Friedman AK, Juarez B, Ku SM, Koo JW, et al. (2013): Rapid regulation of depression-related behaviours by control of midbrain dopamine neurons. *Nature*. 493:532–536. [PubMed: 23235832]
11. Friedman AK, Walsh JJ, Juarez B, Ku SM, Chaudhury D, Wang J, et al. (2014): Enhancing depression mechanisms in midbrain dopamine neurons achieves homeostatic resilience. *Science (New York, NY)*. 344:313–319.
12. Dias C, Feng J, Sun H, Shao NY, Mazei-Robison MS, Dames-Werno D, et al. (2014): beta-catenin mediates stress resilience through Dicer1/microRNA regulation. *Nature*. 516:51–55. [PubMed: 25383518]
13. Walsh JJ, Friedman AK, Sun H, Heller EA, Ku SM, Juarez B, et al. (2014): Stress and CRF gate neural activation of BDNF in the mesolimbic reward pathway. *Nature neuroscience*. 17:27–29. [PubMed: 24270188]
14. Mandalaywala TM, Petruccio LA, Parker KJ, Maestripieri D, Higham JP (2017): Vigilance for threat accounts for inter-individual variation in physiological responses to adversity in rhesus macaques: A cognition x environment approach. *Developmental psychobiology*. 59:1031–1038. [PubMed: 29071705]
15. Carter ME, Yizhar O, Chikahisa S, Nguyen H, Adamantidis A, Nishino S, et al. (2010): Tuning arousal with optogenetic modulation of locus coeruleus neurons. *Nature neuroscience*. 13:1526–1533. [PubMed: 21037585]
16. Wagatsuma A, Okuyama T, Sun C, Smith LM, Abe K, Tonegawa S (2018): Locus coeruleus input to hippocampal CA3 drives single-trial learning of a novel context. *Proceedings of the National Academy of Sciences of the United States of America*. 115:E310–e316. [PubMed: 29279390]
17. Carter ME, Brill J, Bonnavion P, Huguenard JR, Huerta R, de Lecea L (2012): Mechanism for Hypocretin-mediated sleep-to-wake transitions. *Proceedings of the National Academy of Sciences of the United States of America*. 109:E2635–2644. [PubMed: 22955882]
18. Cao JL, Vialou VF, Lobo MK, Robison AJ, Neve RL, Cooper DC, et al. (2010): Essential role of the cAMP-response-element binding protein pathway in opiate-induced homeostatic adaptations of locus coeruleus neurons. *Proceedings of the National Academy of Sciences of the United States of America*. 107:17011–17016. [PubMed: 20837544]
19. Krystal JH, Neumeister A (2009): Noradrenergic and serotonergic mechanisms in the neurobiology of posttraumatic stress disorder and resilience. *Brain Res*. 13:13–23.
20. Valentino RJ, Van Bockstaele E (2015): Endogenous Opioids: The Downside of Opposing Stress. *Neurobiol Stress*. 1:23–32. [PubMed: 25506603]
21. Isingrini E, Perret L, Rainer Q, Amilhon B, Guma E, Tanti A, et al. (2016): Resilience to chronic stress is mediated by noradrenergic regulation of dopamine neurons. *Nature neuroscience*. 19:560–563. [PubMed: 26878672]

22. Rothbauer U, Zolghadr K, Tillib S, Nowak D, Schermelleh L, Gahl A, et al. (2006): Targeting and tracing antigens in live cells with fluorescent nanobodies. *Nat Methods*. 3:887–889. [PubMed: 17060912]
23. Ekstrand MI, Nectow AR, Knight ZA, Latcha KN, Pomeranz LE, Friedman JM (2014): Molecular profiling of neurons based on connectivity. *Cell*. 157:1230–1242. [PubMed: 24855954]
24. Nectow AR, Ekstrand MI, Friedman JM (2015): Molecular characterization of neuronal cell types based on patterns of projection with Retro-TRAP. *Nat Protoc*. 10:1319–1327. [PubMed: 26247298]
25. Cao JL, Covington HE 3rd, Friedman AK, Wilkinson MB, Walsh JJ, Cooper DC, et al. (2010): Mesolimbic dopamine neurons in the brain reward circuit mediate susceptibility to social defeat and antidepressant action. *The Journal of neuroscience : the official journal of the Society for Neuroscience*. 30:16453–16458. [PubMed: 21147984]
26. Berton O, McClung CA, Dileone RJ, Krishnan V, Renthal W, Russo SJ, et al. (2006): Essential role of BDNF in the mesolimbic dopamine pathway in social defeat stress. *Science (New York, NY)*. 311:864–868.
27. Torrecilla M, Fernandez-Aedo I, Arrue A, Zumarraga M, Ugedo L (2013): Role of GIRK channels on the noradrenergic transmission in vivo: an electrophysiological and neurochemical study on GIRK2 mutant mice. *Int J Neuropsychopharmacol*. 16:1093–1104. [PubMed: 23040084]
28. Gobbi G, Cassano T, Radja F, Morgese MG, Cuomo V, Santarelli L, et al. (2007): Neurokinin 1 receptor antagonism requires norepinephrine to increase serotonin function. *Eur Neuropsychopharmacol*. 17:328–338. [PubMed: 16950604]
29. Doyle JP, Dougherty JD, Heiman M, Schmidt EF, Stevens TR, Ma G, et al. (2008): Application of a translational profiling approach for the comparative analysis of CNS cell types. *Cell*. 135:749–762. [PubMed: 19013282]
30. Aston-Jones G, Cohen JD (2005): An integrative theory of locus coeruleus-norepinephrine function: adaptive gain and optimal performance. *Annu Rev Neurosci*. 28:403–450. [PubMed: 16022602]
31. Nestler EJ, Aghajanian GK (1997): Molecular and cellular basis of addiction. *Science (New York, NY)*. 278:58–63.
32. Han MH, Bolanos CA, Green TA, Olson VG, Neve RL, Liu RJ, et al. (2006): Role of cAMP response element-binding protein in the rat locus ceruleus: regulation of neuronal activity and opiate withdrawal behaviors. *The Journal of neuroscience : the official journal of the Society for Neuroscience*. 26:4624–4629. [PubMed: 16641242]
33. Covington HE 3rd, Lobo MK, Maze I, Vialou V, Hyman JM, Zaman S, et al. (2010): Antidepressant effect of optogenetic stimulation of the medial prefrontal cortex. *J Neurosci*. 30:16082–16090. [PubMed: 21123555]
34. Bagot RC, Parise EM, Pena CJ, Zhang HX, Maze I, Chaudhury D, et al. (2015): Ventral hippocampal afferents to the nucleus accumbens regulate susceptibility to depression. *Nat Commun*. 6.
35. Friedman AK, Juarez B, Ku SM, Zhang H, Calizo RC, Walsh JJ, et al. (2016): KCNQ channel openers reverse depressive symptoms via an active resilience mechanism. *Nature communications*. 7:11671.
36. Zhang H, Chaudhury D, Juarez B, Friedman A, Ku S, Nectow A, et al. (2015): Role of Locus Coeruleus-Ventral Tegmental Area Circuit in Mediating the Resilience to Social Stress. *Neuropsychopharmacology : official publication of the American College of Neuropsychopharmacology: NATURE PUBLISHING GROUP MACMILLAN BUILDING, 4 CRINAN ST, LONDON N1 9XW, ENGLAND*, pp S237–S238.
37. Paladini CA, Williams JT (2004): Noradrenergic inhibition of midbrain dopamine neurons. *The Journal of neuroscience : the official journal of the Society for Neuroscience*. 24:4568–4575. [PubMed: 15140928]
38. Arencibia-Albite F, Paladini C, Williams JT, Jimenez-Rivera CA (2007): Noradrenergic modulation of the hyperpolarization-activated cation current (I_h) in dopamine neurons of the ventral tegmental area. *Neuroscience*. 149:303–314. [PubMed: 17884297]

39. Sara SJ (2009): The locus coeruleus and noradrenergic modulation of cognition. *Nature reviews Neuroscience*. 10:211–223. [PubMed: 19190638]
40. Krystal JH, Neumeister A (2009): Noradrenergic and serotonergic mechanisms in the neurobiology of posttraumatic stress disorder and resilience. *Brain research*. 1293:13–23. [PubMed: 19332037]
41. Valentino RJ, Foote SL, Page ME (1993): The locus coeruleus as a site for integrating corticotropin-releasing factor and noradrenergic mediation of stress responses. *Annals of the New York Academy of Sciences*. 697:173–188. [PubMed: 7903030]
42. Koob GF (1999): Corticotropin-releasing factor, norepinephrine, and stress. *Biological psychiatry*. 46:1167–1180. [PubMed: 10560023]
43. Nestler EJ, Alreja M, Aghajanian GK (1999): Molecular control of locus coeruleus neurotransmission. *Biological psychiatry*. 46:1131–1139. [PubMed: 10560020]
44. Reyes BA, Bangasser DA, Valentino RJ, Van Bockstaele EJ (2014): Using high resolution imaging to determine trafficking of corticotropin-releasing factor receptors in noradrenergic neurons of the rat locus coeruleus. *Life sciences*. 112:2–9. [PubMed: 25058917]
45. Bingham B, McFadden K, Zhang X, Bhatnagar S, Beck S, Valentino R (2011): Early adolescence as a critical window during which social stress distinctly alters behavior and brain norepinephrine activity. *Neuropsychopharmacology : official publication of the American College of Neuropsychopharmacology*. 36:896–909. [PubMed: 21178981]
46. McCall JG, Al-Hasani R, Siuda ER, Hong DY, Norris AJ, Ford CP, et al. (2015): CRH Engagement of the Locus Coeruleus Noradrenergic System Mediates Stress-Induced Anxiety. *Neuron*. 87:605–620. [PubMed: 26212712]
47. Schwarz LA, Miyamichi K, Gao XJ, Beier KT, Weissbourd B, DeLoach KE, et al. (2015): Viral-genetic tracing of the input-output organization of a central noradrenaline circuit. *Nature*. 524:88–92. [PubMed: 26131933]
48. Waterhouse BD, Chandler DJ Heterogeneous organization and function of the central noradrenergic system. *Brain Res*. 2015 12 30. pii: S0006-8993(15)00989-0. doi: 10.1016/j.brainres.2015.12.050.
49. Schwarz LA, Luo L (2015): Organization of the locus coeruleus-norepinephrine system. *Current biology : CB*. 25:R1051–1056. [PubMed: 26528750]
50. Lammel S, Hetzel A, Hackel O, Jones I, Liss B, Roeper J (2008): Unique properties of mesoprefrontal neurons within a dual mesocorticolimbic dopamine system. *Neuron*. 57:760–773. [PubMed: 18341995]
51. Lammel S, Lim BK, Ran C, Huang KW, Betley MJ, Tye KM, et al. (2012): Input-specific control of reward and aversion in the ventral tegmental area. *Nature*. 491:212–217. [PubMed: 23064228]
52. Naegeli C, Zeffiro T, Piccirelli M, Jaillard A, Weilenmann A, Hassanpour K, et al. (2018): Locus Coeruleus Activity Mediates Hyperresponsiveness in Posttraumatic Stress Disorder. *Biological psychiatry*. 83:254–262. [PubMed: 29100627]
53. Anyan J, Amir S (2018): Too Depressed to Swim or Too Afraid to Stop? A Reinterpretation of the Forced Swim Test as a Measure of Anxiety-Like Behavior. *Neuropsychopharmacology : official publication of the American College of Neuropsychopharmacology*. 43:931–933. [PubMed: 29210364]
54. Krystal JH, Sanacora G, Duman RS (2013): Rapid-acting glutamatergic antidepressants: the path to ketamine and beyond. *Biological psychiatry*. 73:1133–1141. [PubMed: 23726151]
55. Donahue RJ, Muschamp JW, Russo SJ, Nestler EJ, Carlezon WA Jr. (2014): Effects of striatal DeltaFosB overexpression and ketamine on social defeat stress-induced anhedonia in mice. *Biological psychiatry*. 76:550–558. [PubMed: 24495460]

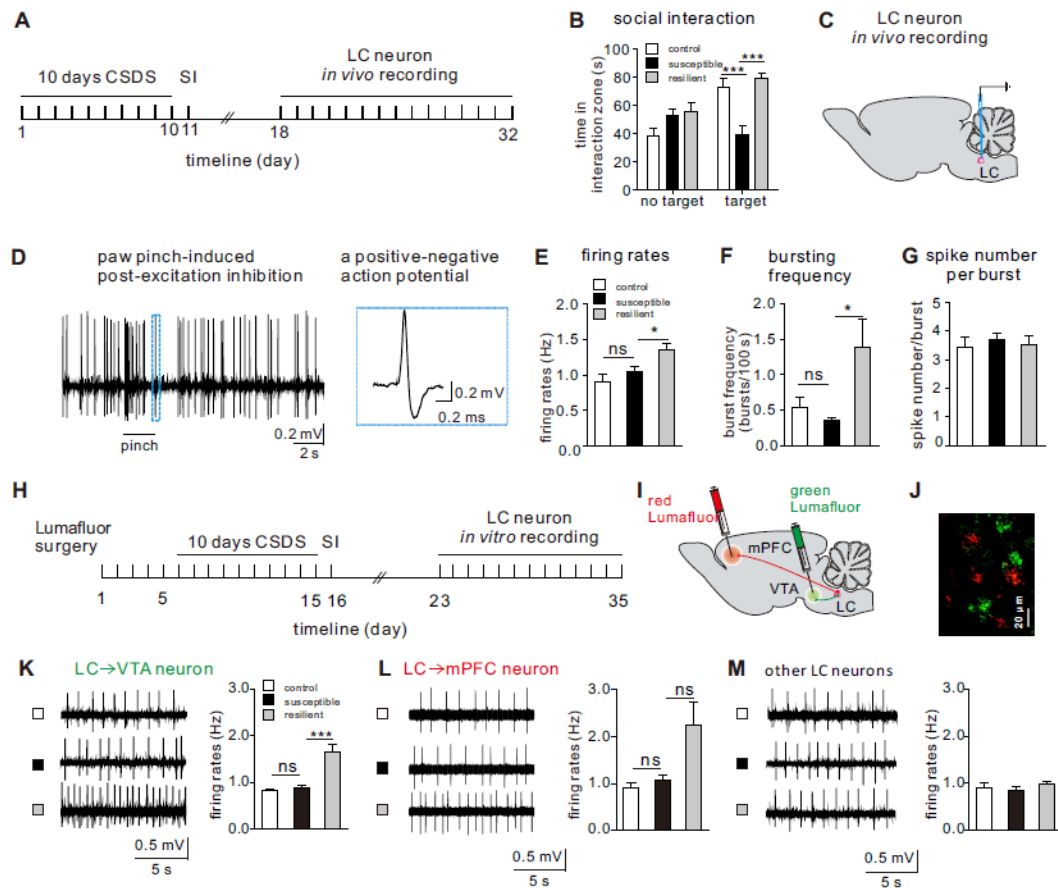
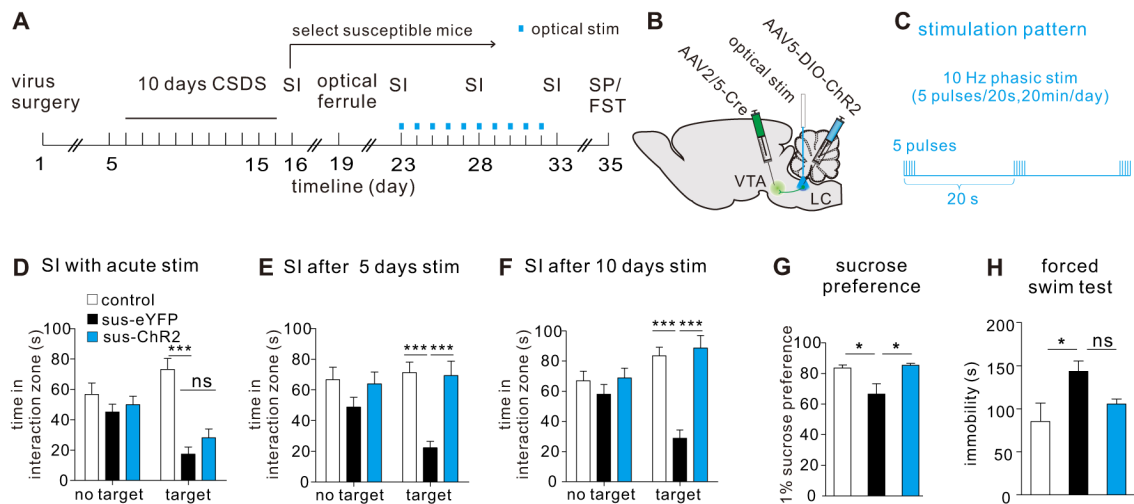


Figure 1.

LC→VTA circuit neurons display increased firing activity selectively in resilient mice. **(A)** Experimental timeline of CSDS, social interaction (SI), and *in vivo* single-unit recording experiments. **(B)** SI measures on day 11 showing the significantly decreased social interaction time in susceptible mice (*two-way ANOVA*, $F_{2,52}=11.19$, $P<0.0001$, *post-hoc Bonferroni's test*: control vs. susceptible, *** $P=0.0002$, susceptible vs. resilient, *** $P<0.0001$, $n=9-10$ mice/group). **(C)** Schematic showing *in vivo* single-unit recordings. **(D)** Sample traces showing foot pinch-induced post-excitation inhibition and a typical action potential of an LC NE neuron. **(E)** Increased firing rates of LC neurons in the resilient mice (*one-way ANOVA*, $F_{2,91}=6.38$, $P=0.0026$, *post-hoc Bonferroni's test*: control vs. susceptible, $P=0.91$, susceptible vs. resilient, * $P=0.0342$, $n=21-39$ cells/6-8 mice/group). **(F)** Increased burst frequencies/100 s of LC neurons in the resilient mice (*one-way ANOVA*, $F_{2,79}=3.94$, $P=0.0233$, *post-hoc Bonferroni's test*: control vs. susceptible, $P>0.9999$, susceptible vs. resilient, * $P=0.026$, $n=17-33$ cells/6-8 mice/group). **(G)** No significant difference was observed in spike number/burst between groups (*Dunn's multiple comparisons test*: control vs. susceptible, $P>0.9999$, susceptible vs. resilient, $P=0.4969$, $n=17-33$ cells/6-8 mice/group). **(H)** Experimental timeline of *ex vivo* pathway-specific cell-attached recordings. **(I)** Schematic showing retrograde Lumaflluors injected into mPFC and VTA. **(J)** Lumaflluor-labeled LC neurons (Green: LC→VTA neurons, Red: LC→mPFC neurons). **(K)** Sample traces of neuronal firing, and quantitative data showing the

significantly increased LC→VTA neuron firing rates of the resilient mice (*one-way ANOVA*, $F_{2, 40}=13.46$, $P<0.0001$, *post-hoc Bonferroni's test*: control vs. susceptible, $P>0.9999$, susceptible vs. resilient, $P<0.0001$, $n=8-20$ cells/4 mice/group). **(L)** Sample traces of neuronal firing, and quantitative data showing no difference in LC→mPFC neuron firing rates between groups (*Dunn's multiple comparisons test*: control vs. susceptible, $P=0.7882$, susceptible vs resilient, $P=0.2257$, $n=10-23$ cells/4 mice/group). **(M)** Sample traces of neuronal firing, and quantitative data showing no difference in unlabeled LC neuron firing rates between groups (*Dunn's multiple comparisons test*: control vs. susceptible, $P>0.9999$, susceptible vs resilient, $P>0.9999$, $n=9-23$ cells/4 mice/group). Error bars indicate mean \pm s.e.m. ns: no significance.

**Figure 2.**

Repeated optogenetic activation of LC→VTA neurons promotes resilience in previously defined susceptible mice. **(A)** Experimental timeline of surgeries, CSDS, SI, optical stimulation, sucrose preference (SP) and forced swim test (FST). **(B)** Schematic showing viral surgeries and optical stimulation. **(C)** Optical phasic stimulation pattern. **(D)** No significant difference was observed in social interaction time during optical stimulation between sus-eYFP group and sus-ChR2 group (*two-way ANOVA*, $F_{2,124}=6.562$, $P=0.002$, *post-hoc Bonferroni's test*, control vs. sus-eYFP, $***P<0.0001$, sus-eYFP vs. sus-ChR2, $P>0.9999$, $n=21-23$ mice/group). **(E)** Increased social interaction time after 5 days of repeated optical stimulation in sus-ChR2 group (*two-way ANOVA*, $F_{2,122}=3.114$, $P=0.0479$, *post-hoc Bonferroni's test*, control vs. sus-eYFP, $***P<0.0001$, sus-eYFP vs. sus-ChR2, $***P<0.0001$, $n=20-23$ mice/group). **(F)** Increased social interaction time after 10 days of repeated optical stimulation in sus-ChR2 group (*two-way ANOVA*, $f_{2,124}=8.696$, $P=0.0003$, *post-hoc Bonferroni's test*, control vs. sus-eYFP, $***P<0.0001$, sus-eYFP vs. sus-ChR2, $***P<0.0001$, $n=21-23$ mice/group). **(G)** Increased sucrose preference after 10 days of repeated optical stimulation in sus-ChR2 group (*one-way ANOVA*, $F_{2,18}=6.29$, $P=0.0085$, *post-hoc Bonferroni's test*, control vs. sus-eYFP, $*P=0.0381$, sus-eYFP vs. sus-ChR2, $*P=0.012$, $n=6-8$ mice/group). **(H)** No significant changes were observed in immobility time in forced swim test after 10 days of repeated optical stimulation between groups (*Dunn's multiple comparisons test*: control vs. sus-eYFP, $*P=0.0340$, sus-eYFP vs. sus-ChR2, $P=0.0563$, $n=5-8$ mice/group). Error bars indicate mean \pm s.e.m. ns: no significance.

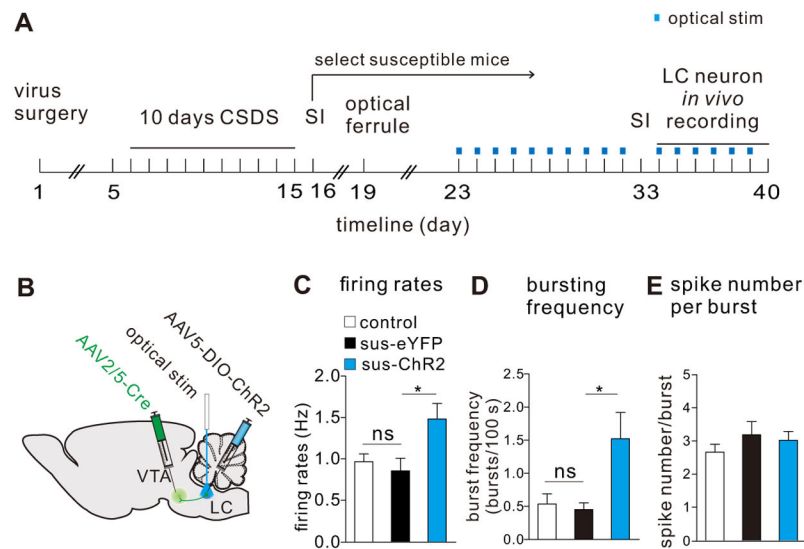


Figure 3.

Repeated optical activation of LC→VTA neurons in susceptible mice enhances the firing activity of LC neurons. **(A)** Experimental timeline for *in vivo* single-unit recordings following repeated stimulation of LC→VTA neurons. **(B)** Schematic showing surgeries for virus injections and optical stimulation of LC→VTA neurons. **(C)** Increased LC neuron firing rates after 10 days of repeated optical stimulation in sus-ChR2 group (*one-way ANOVA*, $F_{2,84}=4.82$, $P=0.0104$, *post-hoc Bonferroni's test*: control vs sus-eYFP, $P>0.9999$, sus-eYFP vs sus-ChR2, $*P=0.0484$, $n=14-41$ cells/4-7 mice/group). **(D)** Increased LC neuron bursting frequencies/100 s after 10 days of repeated optical stimulation in sus-ChR2 group (*one-way ANOVA*, $F_{2,40}=5.06$, $P=0.011$, *post-hoc Bonferroni's test*: control vs sus-eYFP, $P>0.999$, sus-eYFP vs sus-ChR2, $*P=0.0433$, $n=9-20$ cells/4-7 mice/group). **(E)** No difference was observed in LC neuron spike number/burst between groups (*one-way ANOVA*, $F_{2,40}=0.90$, $P=0.4154$, *post-hoc Bonferroni's test*: control vs sus-eYFP, $P=0.6921$, sus-eYFP vs sus-ChR2, $P>0.9999$, $n=9-20$ cells/4-7 mice/group). Error bars indicate mean \pm s.e.m.

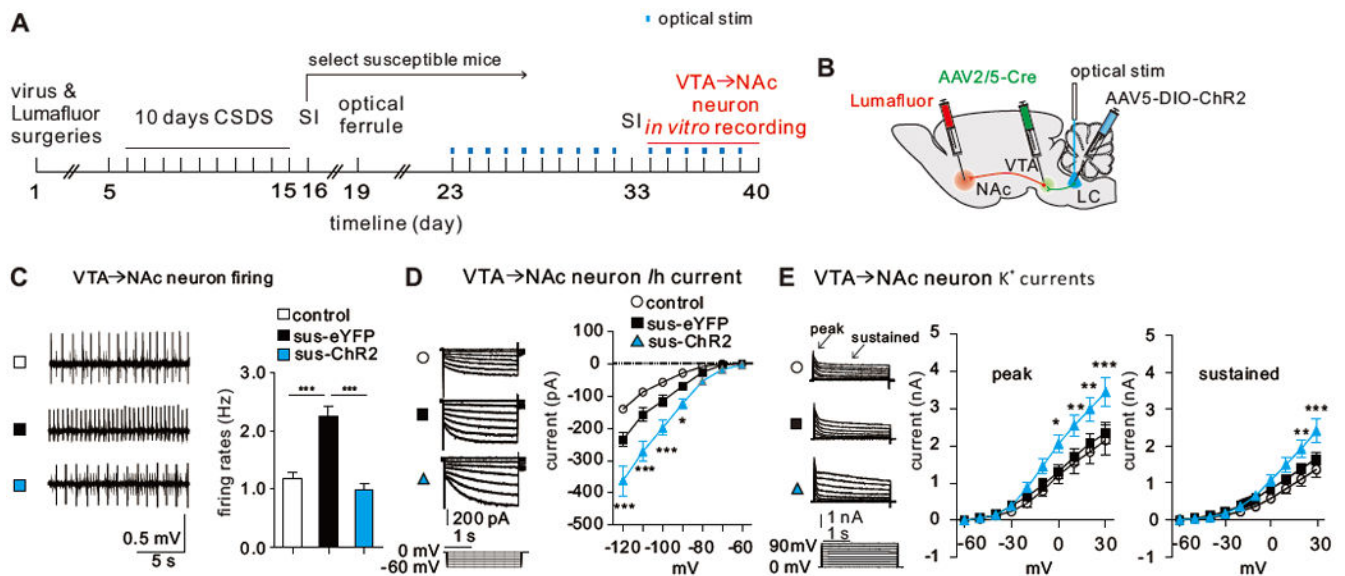


Figure 4.

Repeated optical activation of LC->VTA neurons in susceptible mice induces homeostatic plasticity in VTA->NAc DA neurons. **(A)** Experimental timeline. **(B)** Schematic showing surgeries for Lumafluor and virus injections, and optical stimulation of LC->VTA neurons. **(C)** Sample traces of neuronal firing, and quantitative data showing the significantly decreased VTA->NAc neuron firing rates after 10 days of repeated optical stimulation in sus-ChR2 group (*one-way ANOVA*, $F_{2,39}=26.39$, $P<0.0001$, control vs. sus-eYFP, $***P<0.0001$; sus-eYFP vs. sus-ChR2, $***P<0.001$; $n=12-17$ cells/6-8 mice). **(D)** I_h current sample traces, and quantitative data showing the increased I_h currents in VTA->NAc neurons after 10 days of repeated optical stimulation in sus-ChR2 group (*two-way ANOVA*, $F_{12,231}=9.04$, $P<0.001$, *post-hoc Bonferroni's test*: sus-eYFP vs. sus-chR2, at -120 mV, $***P<0.0001$, at -110 mV, $***P<0.0001$, at -100 mV, $***P=0.0003$, at -90 mV, $*P=0.03$; $n=9-15$ cells/6-8 mice/group). **(E)** K^+ currents sample traces, and quantitative data showing increased K^+ currents in VTA->NAc neurons after 10 days of repeated optical stimulation in sus-ChR2 group (Peak: *two-way ANOVA*, $F_{18,289}=1.98$, $P<0.0001$; *post-hoc Bonferroni's test*: sus-eYFP vs. sus-chR2, at 30 mV, $***P=0.0003$, at 20 mV, $**P=0.0026$, at 10 mV, $**P=0.0073$, at 0 mV, $*P=0.0203$; $n=9-13$ cells/6-8 mice/group; Sustained: *two-way ANOVA*, $F_{18,289}=2.62$, $P<0.0001$, *post-hoc Bonferroni's test*: sus-eYFP vs. sus-chR2, at 30 mV, $***P<0.0001$, at 20 mV, $**P=0.0059$, $n=9-13$ cells/6-8 mice/group). Error bars indicate mean \pm s.e.m.

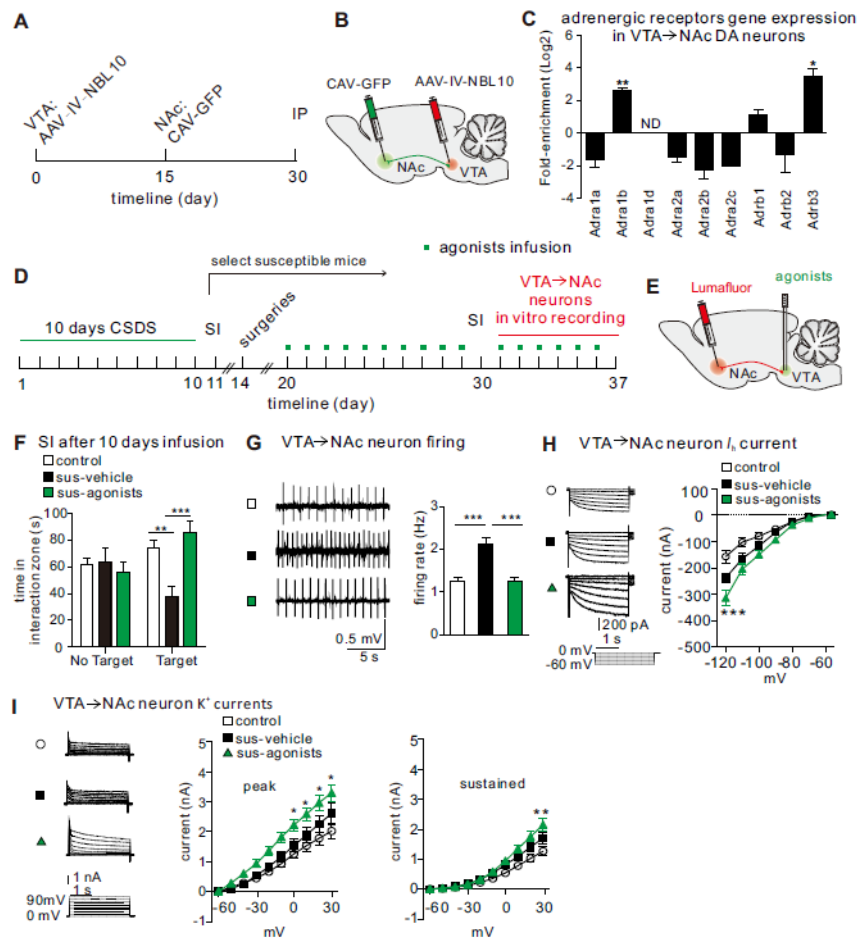


Figure 5. Activation of $\alpha 1$ and $\beta 3$ adrenergic receptors is sufficient to induce resilience. (**A**, **B**) Experimental timeline and schematic for examination of VTA→NAc pathway-specific adrenergic receptor genes. (**C**) Higher fold-enrichment of adrenergic receptors on VTA→NAc DA neurons (normalized to overall VTA DA neurons; enriched genes: *Adra1b*, $t_2=24.80$, $**P=0.0016$; and *Adrb3*, $t_2=7.808$, $*P=0.016$, $n=3$ groups/6 mice/group). ND, not detected in IP. (**D**) Experimental timeline. (**E**) Schematic showing agonists infusion and Lumafluor injection to label VTA→NAc neurons. (**F**) Increased social interaction time after 10 days of agonists infusion in sus-agonists group (*two-way ANOVA*, $F_{2,54}=6.966$, $P=0.002$, $n=9-12$ mice/group, *post-hoc Bonferroni's test*: control vs. sus-vehicle, $**P=0.0023$; sus-vehicle vs. sus-agonists, $***P=0.0003$). (**G**) Sample traces of neuronal firing, and quantitative data showing the significantly decreased VTA→NAc neuron firing rates after 10 days of agonists infusion in sus-agonists group (*one-way ANOVA*, $F_{2,63}=22.72$, $***P<0.0001$, *post-hoc Bonferroni's test*: control vs. sus-vehicle, $***P<0.0001$; sus-vehicle vs. sus-agonists, $***P<0.0001$, $n=19-24$ cells/9-12 mice/group). (**H**) I_h current sample traces, and quantitative data showing the increased I_h currents in VTA→NAc neurons after 10 days of agonists infusion in sus-ChR2 group (*two-way ANOVA*, $F_{12,420}=4.53$, $P<0.0001$, *post-hoc Bonferroni's test*: control vs. sus-vehicle, $***P=0.0006$; sus-vehicle vs. sus-agonists, $***P=0.005$, $n=17-26$ cells/9-12 mice/group). (**I**) K^+ current sample traces, and

quantitative data showing the increased K^+ currents in VTA→NAc neurons after 10 days of agonists infusion in sus-ChR2 group (Peak: *two-way ANOVA*, $F_{18,430}=1.79$, $P=0.0243$, *post-hoc Bonferroni's test*: sus-vehicle vs. sus-agonists, at 30mV, $*P=0.0154$; at 20mV, $*P=0.0113$; at 10mV, $*P=0.0141$; at -10mV, $*P=0.0235$, $n=14-17$ cells/9-12 mice/group; Sustained: *two-way ANOVA*, $F_{18,430}=3.62$, $P<0.0001$, *post-hoc Bonferroni's test*: sus-vehicle vs. sus-agonists, at 30mV, $**P=0.0012$; $n=14-17$ cells/9-12 mice/group). Error bars indicate mean \pm s.e.m.

Author Manuscript

Author Manuscript

Author Manuscript

Author Manuscript

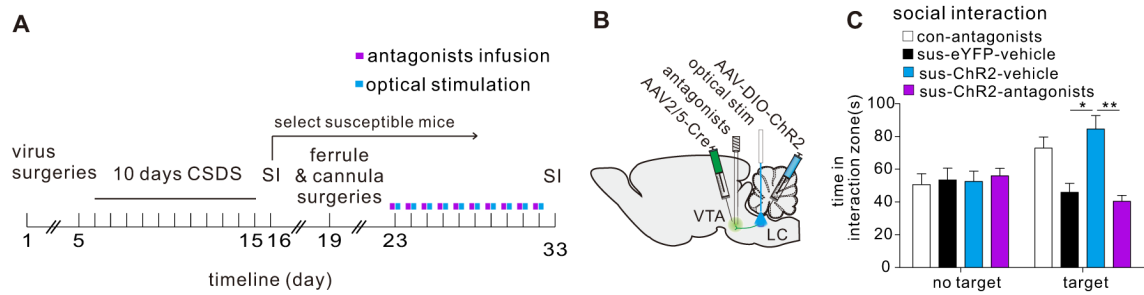


Fig. 6.

VTA α_1 and β_3 adrenergic receptors are necessary to the pro-resilience effect of repeated optical stimulation. **(A)** Schematic showing virus surgeries, antagonist infusion and optical stimulation. **(B)** Experimental timeline. **(C)** Increased social interaction time induced by repeated optical stimulation was blocked by 10 days of intra-VTA pretreatment with α_1 and β_3 receptor antagonists (two-way ANOVA, $F_{3,42}=6.332$, $P=0.0012$, *post-hoc Bonferroni's test*: sus-eYFP-vehicle vs. sus-ChR2-vehicle, $P=0.0435$; sus-ChR2-vehicle vs. sus-ChR2-antagonists, $*P=0.0157$, $n=6-7$ mice/group). Error bars indicate mean \pm s.e.m.